

Sparse component separation from Poisson measurements

I. El Hamzaoui and J. Bobin.

IRFU, CEA, Université Paris-Saclay, F-91191 Gif-sur-Yvette, France

Abstract— Blind source separation (BSS) aims at recovering signals from mixtures. This problem has been extensively studied in cases where the mixtures are contaminated with additive Gaussian noise. However, it is not well suited to describe data that are corrupted with Poisson measurements such as in low photon count optics or in high-energy astronomical imaging (e.g. observations from the Chandra or Fermi telescopes). To that purpose, we propose a novel BSS algorithm coined pGMCA that specifically tackles the blind separation of sparse sources from Poisson measurements.

Introduction

Multichannel data are composed of m observations \mathbf{X}_i , each of which is made of t samples. According to the standard instantaneous linear mixture, each observation is described as a linear combination of n elementary sources or components \mathbf{S}_j . It is classically assumed that the data are corrupted with additive, generally Gaussian, noise, which leads to the following matrix formulation $\mathbf{X} = \mathbf{AS} + \mathbf{N}$, where $\mathbf{X} \in \mathbb{R}^{m \times t}$ is the observations matrix, $\mathbf{S} \in \mathbb{R}^{n \times t}$ the sources matrix, $\mathbf{A} \in \mathbb{R}^{m \times n}$ the mixing matrix and $\mathbf{N} \in \mathbb{R}^{m \times t}$ for the noise contribution. In this context, BSS aims at recovering both the mixing matrix \mathbf{A} and the sources \mathbf{S} from the data \mathbf{X} only. This is essentially an unsupervised matrix factorization; being ill-posed it requires additional assumptions about the sources and/or mixing matrix such as statistical independence [13], non-negativity [6] or sparsity [9, 2] to only name three. However, the above linear mixture model does not describe precisely data that are commonly found in low photon count imaging, such as in X-ray [1]. For that purpose, one needs to account for the exact statistics of the measurements, which precisely follow a Poisson distribution. Hence, the data \mathbf{X} are only defined statistically from the "pure" mixtures \mathbf{AS} ; the probability for a given sample to take the value $\mathbf{X}_i[t]$ is given by the Poisson law: $\mathcal{P}(\mathbf{X}_i[t] | [\mathbf{AS}]_i[t]) = \frac{e^{-[\mathbf{AS}]_i[t]} [\mathbf{AS}]_i[t]^{\mathbf{X}_i[t]}}}{\mathbf{X}_i[t]!}$, where $[\mathbf{AS}]_i[t]$ is the sample of the matrix \mathbf{AS} located at the i -th row and t -th column. To tackle BSS from Poisson measurements, a straightforward approach consists in maximizing the likelihood of mixture variable. In the case of Poisson statistics, this amounts to minimizing the Kullback-Leibler divergence between the data \mathbf{X} and the mixture model \mathbf{AS} with respect to \mathbf{A} and \mathbf{S} , which has been investigated both in the scope of Independent Component Analysis (ICA - [7]) and Non-negative Matrix Factorization (NMF - [6]) where it generally refers to robust BSS. In the scope of sparse BSS, the sources are assumed to admit a sparse distribution in some signal representation Φ . While sparse BSS has been successful in various applications [4], to the best of our knowledge, this blind separation of *sparse* sources has not been investigated when the data follow a Poisson distribution. We therefore propose a new algorithm coined poisson Generalized Morphological Component Analysis (pGMCA) to tackle sparse BSS from Poisson measurements.

The pGMCA algorithm

In the next, we assume each source admits a sparse representation in some signal representation Φ , which will be assumed to be an orthogonal basis for the sake of simplicity. Next, the sparsity of the sources will be enforced by minimizing their re-weighted ℓ_1 norm as follows:

$$\min_{\mathbf{A} \in \mathcal{C}, \mathbf{S} \geq 0} \|\mathbf{A} \odot \mathbf{S} \Phi^T\|_{\ell_1} + \mathcal{L}(\mathbf{X} | \mathbf{A}, \mathbf{S}), \quad (1)$$

where the matrix \mathbf{A} contains the regularization parameters as well as weights for re-weighted ℓ_1 regularization [15]. The second term is the anti-log likelihood of variables \mathbf{A} and \mathbf{S} : $\mathcal{L}(\mathbf{X} | \mathbf{A}, \mathbf{S}) = \sum_{i,t} [\mathbf{AS}]_i[t] - \mathbf{X}_i[t] \log([\mathbf{AS}]_i[t])$. The convex set \mathcal{C} is the intersection of the positivity constraint $\mathbf{A} \geq 0$ and the multi-dimensional ℓ_2 -ball constraint that enforces each column of the mixing matrix to have a ℓ_2 norm lower than 1 so as to alleviate the scale indeterminacy of the mixture model. The norm $\|\cdot\|_F$ is the Frobenius norm. Optimizing the problem in Eq. 1 raises several challenges:

- **A multi-convex problem:** the problem is non-convex but convex with respect to each variable \mathbf{A} and \mathbf{S} assuming the other one is fixed. Hopefully, several optimization strategies have been proposed so far to tackle multi-convex problem such as the Block-Coordinate-Descent algorithm [16, 12], which sequentially optimizes over each variable independently.

- **Non-differentiability and curvature of the data fidelity term:** the data fidelity term $\mathcal{L}(\mathbf{X} | \mathbf{A}, \mathbf{S})$ is not smooth about 0, which rigorously excludes the use of BCD. Furthermore, its curvature at the vicinity of 0 increases at a hyperbolic rate. Consequently, neglecting the non-differentiability of \mathcal{L} at 0 to use the BCD would yield to a dramatically slow convergence rate. This would be especially true for measurements that correspond to low flux values.

To make use of the BCD, we rather propose to resort to a smooth approximation of \mathcal{L} based on the smoothing technique introduced by Nesterov in [8]. Following Nesterov's approach, a smooth approximate \mathcal{L}_μ of \mathcal{L} can be built from its Fenchel dual \mathcal{L}^* [14]: $\mathcal{L}_\mu(\mathbf{Y}) = \inf_{\mathbf{U}} \langle \mathbf{Y}, \mathbf{U} \rangle - \mathcal{L}^*(\mathbf{U}) - \mu \|\mathbf{U}\|_F^2$. The resulting approximate $\mathcal{L}_\mu(\mathbf{Y})$ is differentiable and its gradient is μ -Lipschitz, which makes the application of BCD possible. The approximate sparse BSS problem to tackle is the following:

$$\min_{\mathbf{A} \in \mathcal{C}, \mathbf{S} \geq 0} \|\mathbf{A} \odot \mathbf{S} \Phi^T\|_{\ell_1} + \mathcal{L}_\mu(\mathbf{X} | \mathbf{A}, \mathbf{S}). \quad (2)$$

Building upon the BCD algorithm, the pGMCA algorithm (e.g. poisson-GMCA) sequentially updates each variable \mathbf{S} and \mathbf{A} ; it is described in Alg.1.

Step 1 of the pGMCA algorithm requires minimizing the sum of a smooth data fidelity term with two extra non-smooth penalization, namely the ℓ_1 norm of the sources in Φ and the positivity constraint. In the general case, this step does not admit a closed-form expression. Therefore, at each iteration k , the estimate $\mathbf{S}^{(k+1)}$ is obtained numerically using an implementation of the Generalised Forward-Backward Splitting (G-FBS)

Algorithm 1 pGMCA algorithm

Initialization (*see below*)**while** $\|\mathbf{A}^{(k+1)} - \mathbf{A}^{(k)}\|_F > \epsilon$ **do**1 - *Estimating* \mathbf{S} *assuming* \mathbf{A} *is fixed*:

$$\mathbf{S}^{(k+1)} = \underset{\mathbf{S} \geq 0}{\text{Argmin}} \|\mathbf{A} \odot \mathbf{S} \Phi^T\|_{\ell_1} + \mathcal{L}_\mu(\mathbf{X}|\mathbf{A}^{(k)}, \mathbf{S})$$

2 - *Estimating* \mathbf{A} *assuming* \mathbf{S} *is fixed*:

$$\mathbf{A}^{(k+1)} = \underset{\mathbf{A} \in \mathcal{C}}{\text{Argmin}} \mathcal{L}_\mu(\mathbf{X}|\mathbf{A}, \mathbf{S}^{(k+1)})$$

end while

algorithm. Similarly, step 2 involves the minimization of \mathcal{L}_μ subject to $\mathbf{A} \in \mathcal{C}$, which does not admit a closed-form expression. Since \mathcal{C} is the intersection of a ℓ_2 -ball with unit norm and the positivity orthant, it can be shown that its proximal operator [5] is explicit. Therefore, step 2 is solved using a FISTA-like algorithm [18]. Practical details of the implementation are described below:

- **Initialization:** The problem in Eq. 2 being multi-convex, the BCD algorithm can be quite sensitive to the initial point. In the next section, the pGMCA algorithm is initialized with the output of GMCA, which generally provides a robust first guess estimate.

- **Regularization parameters:** In practice, the BCD turns out to be quite sensitive to the choice of the regularization parameter. In these preliminary investigations, we did not implement any ℓ_1 re-weighting scheme; the matrix \mathbf{A} is therefore constant for all the entries of a given source and varies from one source to the other. In practice the regularisation parameter λ_i for the i -th source is fixed based on the level of the noise that propagates in a single iteration of the G-FBS. More precisely, it is chosen as $\lambda_i = \tau \cdot \text{MAD}(\nabla_{\mathbf{S}} \mathcal{L}_\mu(\mathbf{A}^{(0)}, \mathbf{S}^{(0)}) \Phi^T)$ where the Median-Absolute-Deviation (MAD) is an empirical estimate of the standard deviation of the noise measured in the gradient in the sparsifying representation. Interestingly, while this is suited for Gaussian noise, such a strategy works quite fine in Poisson case for $\tau = 1$ thanks to the use of a smooth approximation of \mathcal{L} . The smoothing parameter mainly depends on the Poisson density \mathbf{AS} ; a small value will yield a more precise approximation but at the cost of a slower convergence (*i.e.* the gradient step size in step 1 and 2 scales like μ). In the next, it has been set to the mean number of measures counts.

- **Stopping criterion and number of iterations:** The number of iterations is fixed 10000. The algorithm stops when the Frobenius norm between two consecutive estimates of the mixing matrix $\|\mathbf{A}^{(k+1)} - \mathbf{A}^{(k)}\|_F$ is lower than $\epsilon = 10^{-6}$.

Numerical experiments

In this section, numerical experiments are carried out on simulations of astrophysical data that have been generated from real Chandra observations of the Cassiopea A supernova remnants. These data are composed of a linear combination of 3 components (128×128 pixels): synchrotron emission, and 2 redshifted iron emission lines. They are composed of 50 observations. The electromagnetic spectrum of the synchrotron emission follows a power law while the two iron components have Gaussian-shaped spectra, which are the instrumental response of lines at different redshifted, which are representative of these data in the energy band 5000–6000 eV (electron-volt). The sources and their spectra are displayed in Fig. 1.

In this abstract, we investigate the performances of the various component separation methods when the mean flux (mean number of counts) evolves. These methods are GMCA,

pGMCA, β -NMF [6] and β -ICA [7]. In the last two ones, the parameter β of the β -divergence is set to 1 to minimize a Kullback-Leibler divergence, which is well suited for Poisson statistics. Φ is chosen as isotropic undecimated wavelet [19]. Since these methods do not impose similar regularization on the sources, they are more fairly compared based on the quality of estimation of the mixing matrix. For that purpose, we make use of the spectral angular distance (SAD) between the estimated $[\hat{\mathbf{A}}]^j$ and input $[\mathbf{A}^o]^j$ columns of the mixing matrix: $\text{SAD} = \sum_{j=1}^n \cos^{-1}(|\langle [\hat{\mathbf{A}}]^j, [\mathbf{A}^o]^j \rangle|) / n$. The results are displayed in Fig.2; each point is the mean valued of 10 Monte-Carlo simulations with different noise realisations. This figure first shows that the robust ICA and robust NMF methods perform badly; the range of mean flux values (*i.e.* 0.5 to 35) correspond to a rather severe noise level for component separation, which could explain these poor results. For mean flux values larger than 2 (*i.e.* on average a number counts equal to 2 per pixel), GMCA performs satisfactorily and pGMCA yields a gain of about 1 order of magnitude with respect to GMCA. For lower number of counts, it is likely that the noise level is too large to perform a reasonable separation process.

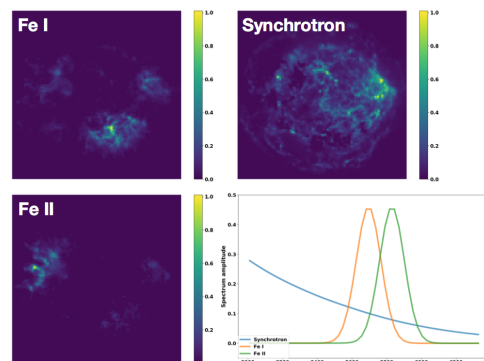


Figure 1: Input sources and their spectra.

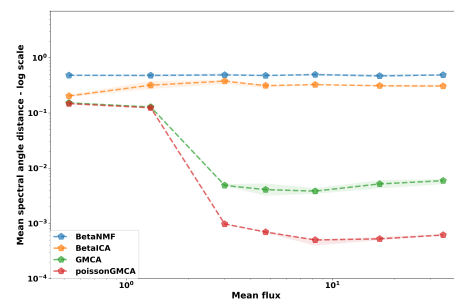


Figure 2: Spectral angular distance as a function of the mean flux.

Conclusion

We investigated the development of a sparsity enforcing method to tackle BSS from measurements with Poisson noise. The proposed pGMCA algorithm builds upon a BCD-like algorithm that makes use a smooth approximation of the Poisson log-likelihood. Preliminary results show a clear improvement of the separation quality with respect to existing methods when the number of counts is low. During the workshop, we will show more extensive results that better highlight the benefits of the proposed pGMCA algorithm.

References

- [1] Badenes, C., X-ray studies of supernova remnants: A different view of supernova explosions, *PNAS*, 107, 16, 2010
- [2] Bobin, J. and Starck, J.-L. and Fadili, J. and Moudden, Y., Sparsity and morphological diversity in blind source separation, *IEEE Transactions on Image Processing*, 16, 11, 2662–2674, 2007
- [3] Bobin, J. and Rapin, J. and Larue, A. and Starck, J.-L., Sparsity and Adaptivity for the Blind Separation of Partially Correlated Sources., *IEEE Transactions on Signal Processing*, 5, 1199–1213, 63, 2015
- [4] Bobin, J. and Sureau, F. and Starck, J.-L., Cosmic microwave background reconstruction from WMAP and Planck PR2 data, *Astronomy & Astrophysics*, A50, 591, 2016
- [5] Combettes, P. and Pesquet, J.-C., Proximal splitting methods in signal processing, *Fixed-point algorithms for inverse problems in science and engineering*, 185–212, 2011
- [6] Févotte, C. and Dobigeon, Ni., Nonlinear hyperspectral unmixing with robust nonnegative matrix factorization, *IEEE Transactions on Image Processing*, 24, 12, 4810–4819, 2015
- [7] Mihoko, M. and Eguchi, S., Robust blind source separation by beta divergence, *Neural computation*, 14, 8, 1859–1886, 2002
- [8] Nesterov, Y., Smooth minimization of non-smooth functions, *Mathematical programming*, 103, 1, 127–152, 2005
- [9] Zibulevsky, M. and Pearlmutter, B., Blind source separation by sparse decomposition in a signal dictionary, *Neural computation*, 13, 4, 863–882, 2001
- [10] Beck, A. and Teboulle, M., A fast iterative shrinkage-thresholding algorithm for linear inverse problems, *SIAM journal on imaging sciences*, 2, 1, 183–202, 2009
- [11] Starck, J.-L. and Fadili, J. and Murtagh, F., *IEEE Transactions on Image Processing*, 2, 297–309, IEEE, The undecimated wavelet decomposition and its reconstruction, 16, 2007
- [12] Xu, Y. and Yin, W., arXiv preprint arXiv:1410.1386, A globally convergent algorithm for nonconvex optimization based on block coordinate update, 2014
- [13] Comon, P. and Jutten, C., Academic Press, *Handbook of Blind Source Separation: Independent component analysis and applications*, 2010
- [14] Rockafellar, T., Princeton University Press, *Princeton Landmarks in Mathematics and Physics, Convex analysis*, 1970
- [15] Candes, E.J. and Wakin, M. B. and Boyd, S. P., *Journal of Fourier Analysis and Applications*, 877–905, 5, Enhancing Sparsity by Reweighted L1 Minimization, 14, 2008
- [16] Tseng, P., *Journal of Optimization Theory and Applications*, 457–494, 3, Convergence of a block coordinate descent method for nondifferentiable minimizations, 109, 2001
- [17] Raguet, H. and Fadili, J. and Peyre, G., *SIAM Journal on Imaging Sciences*, 3, 1199–1226, A Generalized Forward-Backward Splitting, 6, 2013
- [18] Beck, A. and Teboulle, M., *SIAM Imaging Science*, 183–202, Fast iterative shrinkage-thresholding algorithm for linear inverse problems, 2, 2009
- [19] Starck, J.-L. and Fadili, J. and Murtagh, F., *IEEE Transactions on Image Processing*, 2, 297–309, The undecimated wavelet decomposition and its reconstruction, 16, 2007